https://doi.org/10.2352/ISSN.2169-2629.2018.26.67

Using Chromaticity Error Minimisation for Fast Camera Spectral Responsivity Measurement

Andreas Karge; Eberhard Karls University; Tübingen; Germany
Ingmar Rieger; Stuttgart Media University; Stuttgart; Germany
Bernhard Eberhardt; Stuttgart Media University; Stuttgart; Germany
Andreas Schilling; Eberhard Karls University; Tübingen; Germany

Abstract

Measuring the spectral responsivity of a camera using a monochromator is time-consuming and expensive. This work evaluates a fast responsivity measurement method, where diffraction spectrum images are captured and then used for estimating camera responsivity. An error was noticed in the previously proposed measurement method that was caused by spectroradiometer measurement errors and vignetting effects from the camera's lens and sensor. Therefore, a correction step using chromaticity error minimisation is presented to adjust the initial responsivity estimate. It requires a chart to be captured under a known illumination. The chromaticity error of the improved procedure is approximately one order of magnitude smaller than the original error. This enhanced method was employed to create a dataset of spectral responsivities for machine vision, photographic, and movie cameras, which is presented here.

Introduction

The correct display of colours is fundamental in photographic and movie applications, and it is also a requirement in machine vision for colour-based object classification. Uncalibrated camera signals must be converted into a standardised colour domain. A spectral-based colour characterisation of the camera is essential for this conversion. To obtain this, the spectral responsivity of the whole camera system, including lens and filters, must be known. Highly accurate monochromator-based methods exist to estimate the responsitivity of a digital camera. However, they are time consuming and expensive. Therefore, other designs were proposed that use emissive charts, bandpass filters, or filtered light sources in front of the camera [1][2][3]. Several of these methods are discussed and compared to monochromator based-measurement in [4]. All of these methods directly measure the spectral response. Another approach is the capturing of colour chart images to estimate the responsivity. Some of this methods require the knowledge of the spectral power distribution (SPD) of illumination [5], while others estimate response without knowing the SPD of scene lighting as in [6]. A fluorescence-chart-based method is proposed in [7].

An alternative method for measuring the responsivity function of the whole camera system is suggested in [8] as part of Open Film Tools (OFT). It is based on a direct spectral response measurement and allows a fast responsivity estimation with a simplified and inexpensive open source hardware design. This method also requires considerably less measurements and time needed compared to the monochromator method. Figure 1 illustrates a typical measurement setup. OFT-based responsivity measurements also avoid the disadvantage of other methods, like the LED-chart-based procedure, that do not sample all wavelengths. This work evaluates the OFT method. It adds a correction step for estimated responsivity using chromaticity error minimisation. This requires the capture of an additional chart under a known illumination and significantly increases the robustness and quality of the original method. Based on this improvement, a dataset of camera responsivities was created that includes the underlying measurement data.

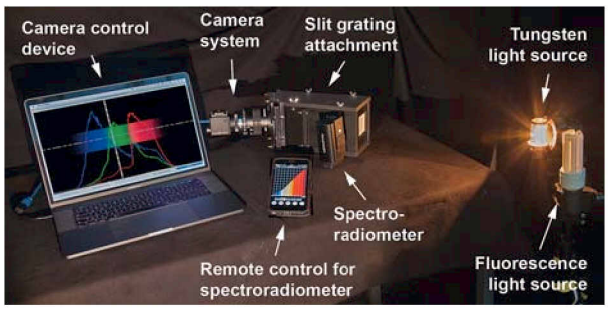

Figure 1. *Typical measurement setup for the Open Film Tools method*

Background

The registered image signal of a camera is a function of the SPD of the illumination $\phi(\lambda_i)$, the spectral reflectance of the object $\rho(\lambda_i)$, and the spectral responsivity $S_{R,G,B}(\lambda_i)$ of the camera RGB channels. Discrete sampled wavelengths are denoted by λ_i. If an object is assumed to be an ideal Lambertian diffuser, and the Fresnel specular highlight reflectance, and optical and electrical cross talk are neglected, then the camera signal can be calculated with equation 1:

$$\vec{C}_{Cam} = \begin{pmatrix} R_{Cam} \\ G_{Cam} \\ B_{Cam} \end{pmatrix} \sim \begin{pmatrix} \sum_{i=1}^{n} \phi(\lambda_i)\rho(\lambda_i)S_R(\lambda_i) \\ \sum_{i=1}^{n} \phi(\lambda_i)\rho(\lambda_i)S_G(\lambda_i) \\ \sum_{i=1}^{n} \phi(\lambda_i)\rho(\lambda_i)S_B(\lambda_i) \end{pmatrix}, \quad (1)$$

with λ_i sampled with $\Delta\lambda$=1nm. The responsivity is influenced by the spectral characteristic of a lens L including mounted filters F having a transmittance $\tau_{LF}(\lambda_i)$, the filter transmittance of the red, green, and blue sensor elements $\tau_{R,G,B}(\lambda_i)$, the infrared cut filter transmittance $\tau_{IR}(\lambda_i)$ and the sensor sensitivity $\sigma(\lambda_i)$ with $S_k(\lambda_i) = \tau_{LF}(\lambda_i)\tau_k(\lambda_i)\tau_{IR}(\lambda_i)\sigma(\lambda_i)$ for k=R,G,B. For a colorimetric application, the uncalibrated pixels sensor signal $\vec{C}_{Cam}$

must be transformed into a standardised colour domain. Since in general, the Luther condition [9] is not fulfilled, this can only be done approximately usually using a 3x3 transformation matrix M, determined by error minimisation:

$$\min_{M} \parallel f_{CAM}(\mathbf{C}^T_{Obs}) - f_{CAM}(\mathbf{C}^T_{Cam}\mathbf{M}^T) \parallel . \quad (2)$$

For the determination of M, a set of reference tristimuli $\mathbf{C}^T_{Obs}$ is used, which is composed of human perception-based colour descriptors, such as CIE-XYZ values for certain object reflectances, while $\mathbf{C}^T_{Cam}$ represents the corresponding set of camera signals. The function f_{CAM} is an optional transformation related to a colour appearance model (CAM). For example, the CIE-XYZ values can be transformed into CIE-Lab76 values. Methods for determining M can be found in [10] and subsequently in [11], [12], [13], and [14]. All these colour characterisation methods require the knowledge of the spectral responsivity of the camera system, which can be obtained with the OFT method. The OFT approach is based on a spectrograph design, where a slit-grating attachment is mounted in front of the camera system. Then the camera captures an image of the whole diffraction spectrum of a light source placed in front of the attachment (Figure 1). The concept of measuring a diffraction spectrum was first presented by J. H. Draper in 1844 [15]. Afterwards his son W. Draper invented the slit-grating-based spectroscope design and used it for applications in astronomy and spectroscopy [16]. While in spectroscopic applications the SPD of the illumination is unknown and calibrated by the known sensor's responsivity, in the OFT method the known SPD of a light source is used to estimate camera responsivity. The underlying concept is also considered as a fast procedure for responsivity estimation for cameras in machine vision [17]. The

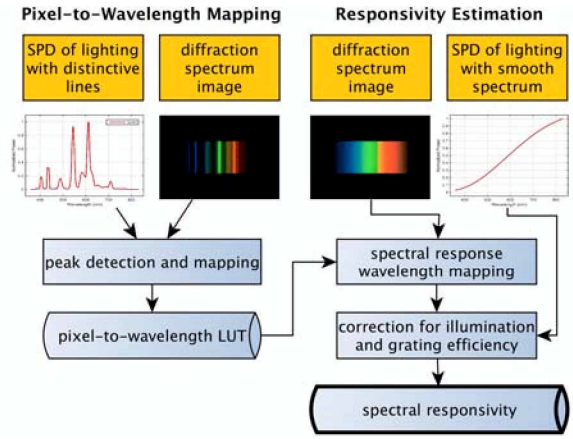

Figure 2. *Overview of the OFT method for responsivity estimation*

OFT method requires two measurement steps. For the first step, the pixel-to-wavelength mapping, a diffraction spectrum image of a light source with distinctive sharp lines must be captured. These lines should be equally distributed over the visible spectrum (VIS: [360 nm, 830 nm]). Before the image is captured, the lines must be vertically aligned in the image plane. The SPD of this light source must also be known or measured. Knowing the wavelengths of the peaks in the spectrum and having measured the pixel coordinates of the corresponding lines in the image, a pixel coordinate to wavelength look up table (LUT) is calculated. In the second step, the responsivity estimation, another diffraction spectrum image is captured using the same alignment. This time, however, a light source with a smooth SPD is used such as a Tungsten light. The image is linearised. Afterwards, the pixel-to-wavelength LUT is applied. Then the responsivity is normalised to the non equal-energy SPD of the lighting, which also must be measured or known. The normalisation also takes the grating efficiency into account, which is the main spectral system parameter of the slit-grating attachment. Figure 2 illustrates an overview of the OFT method.

Evaluation of the OFT method

This section takes a closer look at both measurement steps performed for the OFT method. In particular the reference SPDs and captured diffraction spectrum images for the peak detection as well as the responsivity estimation are discussed in detail. Since the OFT hardware design aims to be a low-budget approach, it is also a requirement to use an inexpensive spectroradiometer. Therefore, the reference SPD measurements are evaluated using a consumer spectroradiometer UPRtek MK350D, and the results are compared to those of a scientific device PhotoResearch PR-670.

Pixel-to-Wavelength Mapping

SPD of Lighting with Distinctive Lines. For the pixel to wavelength mapping step, an OSRAM Duluxe EL Longlife 20 W was used. It is an inexpensive, commonly used fluorescent light that provides distinctive lines. During the evaluation it was found, that the UPRtek must be switched on 30 minutes in advance to obtain correct measurements. This preheating time was used for every measurement with a mandatory dark calibration after preheating. The measured SPDs were evaluated according to short-time stability with samples every 30 second for 10 minutes, and long time stability with samples every second month for 1 year. Table 1 illustrates the drift of the five most powerful lines L_1 to L_5 over time. Peak locations were found to demonstrate both short- and long-time stability. The SPD measurement does not have to be performed for every responsivity estimation. The peak positions are comparable for the UPRtek and the PR-670 measurements having ± 1 nm tolerance.

Table 1. *Mean ($\bar{\lambda}$) and standard deviation (σ_λ) for line peak positions measured with an Uprtek MK350D during a period of one year*

	L_1	L_2	L_3	L_4	L_5
$\bar{\lambda}(nm)$	434.06	488.78	544.84	584.35	612.06
$\sigma_\lambda(nm)$	0.03	0.32	0.00	1.19	0.02

Diffraction Spectrum Image. Specified by the OFT method, line L_3 must be centred and vertically aligned within the image plane. Therefore, the captured image is an effective starting point to investigate lens and sensor vignetting effects. The peak intensity of line L_3 as a function of the vertical distance to the image plane centre, was examined. The signal differs across cameras. Figure 3 illustrates the measured green signals for three different camera models. Several artefacts can be observed: The vertical centre of the slit is not positioned in the image centre due to shift and tilt mounting errors of the slit-grating attachment.

This leads to signal fall-off caused by inclined angles of incidence of light onto a sensor element that changes irradiance in the image plane. Degradation effects caused by lens vignetting effects can also be noticed. Both artefacts attenuate the registered signal resulting in false responsivity estimations. In addition, ripples caused by small slit-width variations[1], but this can be easily averaged out.

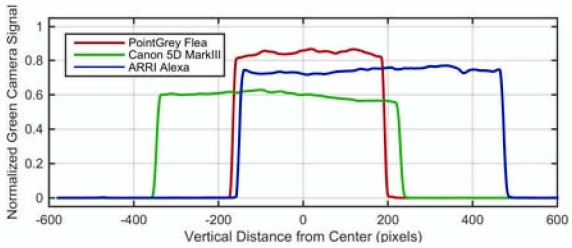

Figure 3. *Vertical green intensity change for the peak of line L_3*

For all camera measurements, the registered outermost lines, L_1 and L_5, were not located at the VIS spectrum range limits but were well inside the range. A linear extrapolation was used to create the pixel coordinate to wavelength mapping for the shorter and longer wavelengths. For a grating with linear dispersion, this is acceptable, if lens distortion is disregarded.

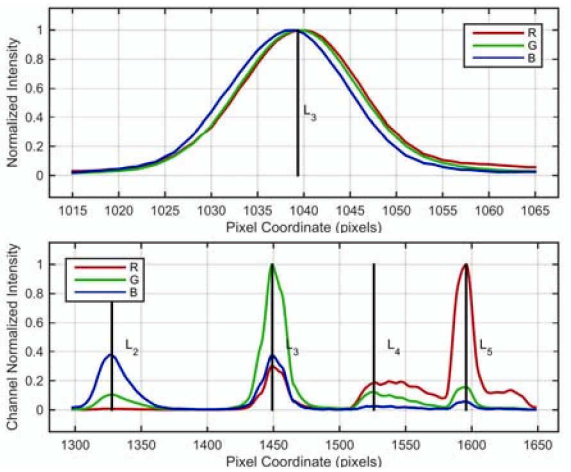

Figure 4. *Camera signals for centred image row: L_3 region for a machine vision camera (top), L_2 to L_5 region for a photographic camera (bottom)*

Two more characteristics were observed that belong together. First, the peak location in general differed in the three RGB channels (Figure 4, top graph). Second the intensity change along the line was asymmetrically degraded (Figure 4, bottom graph). For both, the rationale is that the different slopes of the channel sensitivity functions degrade the original SPD. Steeper slopes result in stronger asymmetric degradations and peak shifts. That results in peak mapping errors that are $\leq 6nm$ for the measured samples. The ripples the right of line L_4 in the bottom graph of Figure 4 show an additional artefact from interference effects between the sensor and the RGB filters, also discussed in [18]. Therefore, the original OFT method was modified by preprocessing the diffraction spectrum image with a Savitzky-Golay filter [19]. This preserved the peak positions while the smoothing avoided detection of local peaks produced by observed interference effects.

Peak Detection and Mapping. Figure 5 shows a sample of mapped peaks in image and reference spectrum for lines L_1 to L_5. For the peak mapping, the image was preprocessed, where the RGB image was converted into a grey image and a mean of the central 200 lines was calculated. The local maxima were detected in both the reference SPD and grey image. For every detected peak, a 2^{nd} degree polynomial was fitted using five additional samples from the peak's neighbourhood. The vertices of the fitted functions from the image where then mapped onto the vertices of the reference SPD resulting in the pixel coordinate to wavelength LUT. For all cameras the outermost blue and red lines of the light source were not registered due to low responsivity in these ranges.

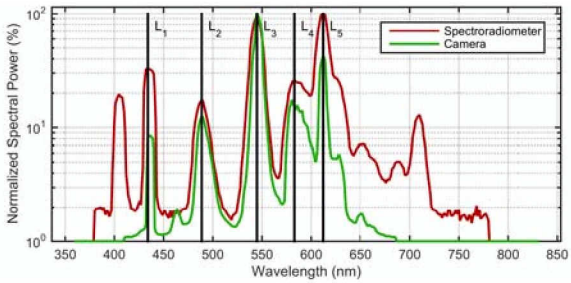

Figure 5. *Mapped lines (vertical black bars) for a Canon 5D Mark III with EF 24-70mm f/2.8L II USM and a UPRtek MK350D*

Responsivity Estimation

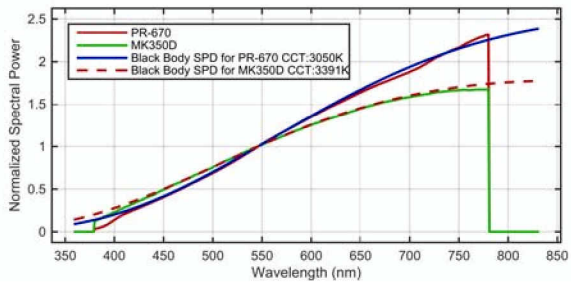

Figure 6. *Tungsten SPD measurements comparison*

SPD of a Smooth Spectrum Lighting. As a spectrally smooth light source, a Dedolight 150 W was chosen for the responsivity estimation step. It is a Tungsten-based lighting, having a correlated colour temperature (CCT) of ≈3400 K. The Tungsten filament is enclosed by a glass tube filled with a mixture of an inert gas and a halogen, and a coated metal mirror is mounted at the backside. The same spectroradiometers from the first measurement step were used. The long- and short-time stability measurements, using the same cycle as before, showed changed SPDs with a CCT variation of ≈100K. Hence, the Tungsten SPD was acquired for every responsivity measurement. The spectrum corresponded approximately to a black-body radiation SPD of the same CCT. In particular, the smoothness was not influenced by

[1]The slit is printed with a 3D printer.

the coated metal mirror. Both spectroradiometers differed slightly in the slope of the linear part of the Tungsten's SPD (Figure 6).

Diffraction Spectrum Image. A mean of the central 200 lines was calculated in each channel in order to average out the influence of slit-width variations. For all measured samples the size of the diffraction spectrum was between 600 and 800 lines wide, such that the geometric optical resolution is at least ≈1nm/pixel. This was one limiting factor for the responsivity resolution.

Normalisation and Response Wavelength Mapping. To obtain normalised camera responsivities, the diffraction spectrum image signals must be normalised by the inverse of the Tungsten SPD (Figure 7, light correction), since no light source with an equal energy SPD is available. Also, the spectral characteristic of the grating, the grating efficiency, attenuates the diffraction spectrum. Therefore, the image was additionally normalised by the inverse of the grating efficiency (Figure 7, grating correction). The complete normalisation of both is shown in Figure 7 as combined correction. This normalization function is almost linear in the middle and long wavelengths of the VIS spectrum with a minimal slope and an almost stable signal to noise ratio. At the lower wavelengths, the correction is dominated by the Tungsten correction term, which is approximately $\sim 1/\lambda$. Hence an initial error in the pixel-to-wavelength LUT leads to an increased error in the estimated response for lower wavelengths.

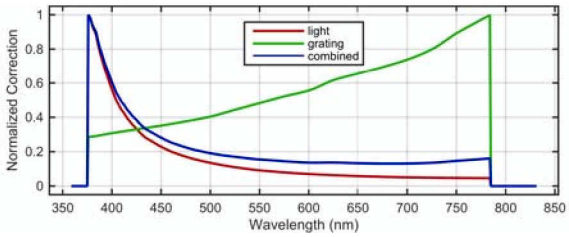

Figure 7. *Responsivity normalisation functions: for light and grating efficiency and the combined correction*

Chromaticity Error Minimisation for the Correction of the Estimated Responsivity

Sources of Error and its Correction. To sum up, the first responsivity estimation given by the OFT method is error-prone. The measured camera systems have a large number of lens and sensor combinations. The size of a diffraction spectrum image generally differs. First, it is biased by three kinds of vignetting effects of the used lenses. These effects can be described using geometrical optics. While for each single lens element the cos^4 law is applicable, the whole lens system is influenced by the pupil aberration given by the aperture diaphragm, as well as by the field stop. These vignetting effects are opposing. The lens design can reduce off-axis fall-off in the periphery to less than cos^4 as discussed in [20]. Sensor element vignetting occurs for all digital cameras. The complete intensity fall-off from the image centre to the periphery can be modelled symmetrically using an even polynomial. One could use a 6^{th} order polynomial as found in [21] to describe the vignetting effect. Second, the measured reference SPD $\tilde{\phi}$ required for the illumination normalisation has an error resulting in different SPD slopes in the measurements of the Tungsten light using different spectroradiometers. Third, the slit-grating attachment influences the measurement, showing shift and tilt errors due to the mounting. And an error in the pixel-to-wavelength LUT leads to an increased error in the estimated response for lower wavelengths. These errors must be corrected. The correction can be introduced to Equation 1, and the registered camera signal for the image using the first estimated response $\tilde{S}$ can thus be written as

$$\tilde{C}_{Cam,k} \sim \sum_{i=1}^{n} f_{spec}(\lambda_i)\tilde{\phi}(\lambda_i)\rho(\lambda_i)f_{\Omega,k}(\lambda_i)f_{vig}(\lambda_i)\tilde{S}_k(\lambda_i). \quad (3)$$

The error corrections are: f_{spec} for the spectroradiometer, f_{vig} for the vignetting, and $f_{\Omega,k}$ for the OFT method. The first two corrections are channel independent. Experiments demonstrated that for the OFT correction a function must be introduced for each channel separately. The signal error of a pixel irradiated by a certain wavelength λ_i is a function of the distance to the centre of the spectrum image. Therefore a parameter r is defined as $r = (\lambda_i - \bar{\lambda})/\Delta\lambda$, where $\Delta\lambda = \hat{\lambda} - \check{\lambda}$ and $\check{\lambda}$ and $\hat{\lambda}$ are respectively the lower and upper VIS range limits. $\bar{\lambda}$ represents the wavelength of the centred line L_3 (Table 1). In the proposed method the error correction functions have been modelled as

$$\begin{aligned} f_{spec}(\lambda_i) &= a_{spec,0} + a_{spec,1}r(\lambda_i), \\ f_{vig}(\lambda_i) &= a_{vig,0} + a_{vig,2}r(\lambda_i)^2, \\ f_{\Omega,k}(\lambda_i) &= a_{\Omega,0,k} + a_{\Omega,1,k}r(\lambda_i) + a_{\Omega,2,k}r(\lambda_i)^2. \end{aligned} \quad (4)$$

$a_{f,p,k}$ are the coefficients for each error correction function f and term p for channel k. Recall that f_{vig} and f_{spec} can be analytically derived approximations, but $f_{\Omega,k}$ is an empirical estimate.

Chromaticity Error Minimisation Step. The first response estimation can be performed in the laboratory and is in essence the OFT method. A further correction step was implemented to reduce these errors. This step requires a captured image of a colour chart under the illumination of a light source with a known SPD (usually in situ). To discard inhomogeneous illumination of the chart and the lens vignetting effects, the intensity independent camera chromaticities for the patches were calculated. A chromaticity is denominated by $\vec{c} = (r,g,b)^T$, where $r = R/(R+G+B), g = G/(R+G+B)$, and $b = B/(R+G+B)$. Then the pixel camera chromaticities for the registered patches represent the expectation values. Applying the originally estimated responsivity, the known reflectances for the patches and the measured illumination SPD to Equation 3 gives the estimated values. The additional correction minimises the error between registered and calculated camera chromaticities.

The complete error correction $\mathbf{f}_{cor}(\lambda_i) = (f_{cor,R}(\lambda_i), f_{cor,G}(\lambda_i), f_{cor,B}(\lambda_i))^T$ corrects the first estimated channel responsivities $\tilde{\mathbf{S}}(\lambda_i) = (\tilde{S}(\lambda_i)_R, \tilde{S}(\lambda_i)_G, \tilde{S}(\lambda_i)_B)^T$ and uses the three error corrections introduced in Equation 4. It is sufficient to consider a 2^{nd} order function as

$$\begin{aligned} f_{cor,k}(\lambda_i) &= a_{0,k} + a_{1,k}r(\lambda_i) + a_{2,k}r(\lambda_i)^2 \\ &\approx f_{spec}(\lambda_i)f_{\Omega,k}(\lambda_i)f_{vig}(\lambda_i)\,. \end{aligned} \quad (5)$$

The coefficients to be estimated for the polynomial are summarized by $\mathbf{a}_k = (a_{0,k}, a_{1,k}, a_{2,k})^T$, $\mathbf{A} = (\mathbf{a}_R, \mathbf{a}_G, \mathbf{a}_B)^T$. Because the chart image might be captured later on using a different white balance, the error minimisation can be scaled for each channel response by the balance $\mathbf{w} = (w_R, w_G, w_B)^T$. The expectation values of the chromaticities are directly calculated from the camera signals of the patches (Cam). The current white balanced

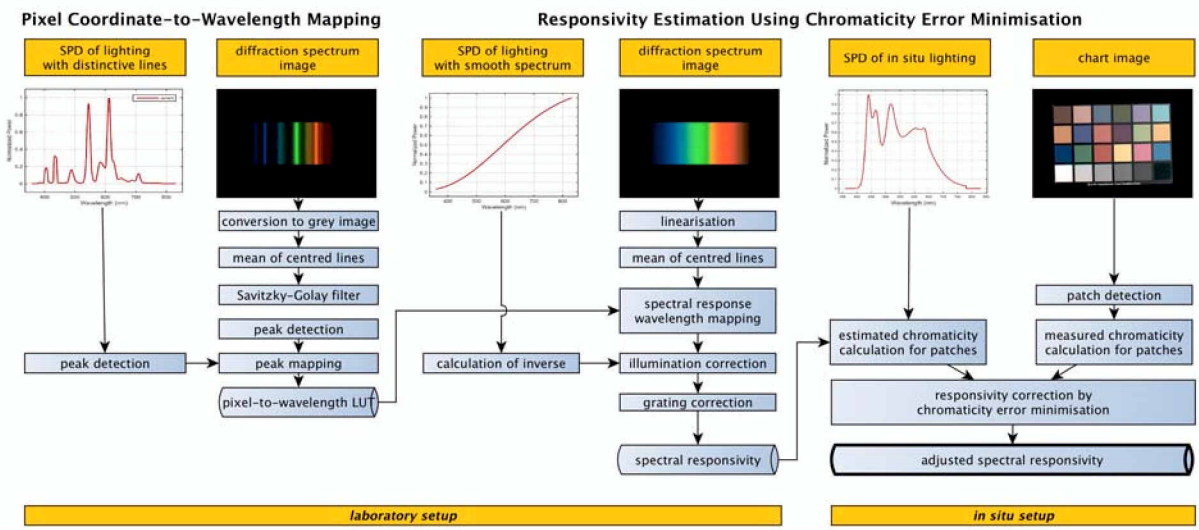

Figure 8. *Proposed method for the estimation of responsivity, with an additional correction using chromaticity error minimisation*

chromaticty values (Est) are calculated by Equation 3, setting $S_k(\lambda_i) = f_{cor,k}(\lambda)\tilde{S}_k$, with k = R,G,B as follows:

$$\vec{c}_{Est} = \frac{diag(\mathbf{w}) \sum_{i=1}^{n} \tilde{\phi}(\lambda_i)\rho(\lambda_i)\mathbf{f}_{cor}(\lambda_i)\tilde{\mathbf{S}}(\lambda_i)}{\sum_{k=R,G,B} w_k \sum_{i=1}^{n} \tilde{\phi}(\lambda_i)\rho(\lambda_i)f_{cor,k}(\lambda_i)\tilde{S}_k(\lambda_i)}, \tag{6}$$

where $\rho(\lambda_i)$ is the spectral patch reflectance. With $\Psi_{\lambda_i} = (\Psi_{R,\lambda_i}, \Psi_{G,\lambda_i}, \Psi_{B,\lambda_i})^T$ and $\Psi_{k,\lambda_i} = \phi(\lambda_i)\rho(\lambda_i)f_{cor,k}(\lambda_i)\tilde{S}_k(\lambda_i)$, the relation between a measured and estimated chromaticity is

$$\vec{c}_{Cam} \sum_{k=R,G,B} w_k \sum_{i=1}^{n} \Psi_{k,\lambda_i} - diag(\mathbf{w}) \sum_{i=1}^{n} \Psi_{\lambda_i} \approx 0. \tag{7}$$

Having the set of chromaticities $\mathbf{c} = \vec{c}_1..\vec{c}_m$ for the number m of patches, the minimisation problem can be stated as

$$\min_{\mathbf{A}} \parallel \mathbf{c}_{Cam}^T - \mathbf{c}_{Est}^T(\mathbf{A}, \mathbf{w}, \tilde{\mathbf{S}}(\lambda_i)) \parallel . \tag{8}$$

This represents a linear equation system with nine unknown coefficients of $\mathbf{A}$. Applying charts, such as a ColorChecker chart with 18 colour patches and the white patch, it becomes an overdetermined linear equation system to be solved by regression due to remaining measurement and modelling errors. The parameter set $\mathbf{A}$ was estimated using the Levenberg-Marquardt algorithm with coefficients initially all set to a value of one. Finally, the initial response $\tilde{\mathbf{S}}$ was scaled by the white balance $\mathbf{w}$ and corrected by $\mathbf{f}_{cor}(\lambda)$ resulting in an adjusted responsivity $\tilde{\mathbf{S}}_a$ as follows:

$$\tilde{\mathbf{S}}_a(\lambda) = diag(\mathbf{w})\mathbf{f}_{cor}(\lambda)\tilde{\mathbf{S}}(\lambda). \tag{9}$$

Figure 8 summarises the improved responsivity estimation method using chromaticity error minimisation. It combines the direct measurement of the spectral response with a chart-image-based response adjustment using a known SPD of the illumination. Since the capturing of the chart image and the spectroradiometer measurement are required anyway for a spectral data-based camera characterisation such as in [14], no additional effort is required as the input data for the method already exists.

Evaluation of Spectral Responsivity

Evaluation Setup. The chromaticity error minimisation was evaluated using all 18 colour patches and the white patch of a ColorChecker chart. The chart was illuminated by different lighting. Figure 9 illustrates the SPDs for the applied Tungsten lighting (T), a Kino Flo Celeb 200 at CCTs of 3400 K (LED_1) and 5500 K (LED_2), and an ARRI Compact 125 (HMI). The SPDs were measured with the UPRtek spectroradiometer. The examined camera was a Canon 5D Mark III with an EF 24-70mm f/2.8L II USM lens setting the focal length to 50 mm. The chart was centred, and the distance to the camera was 1.50 meter. The light was vertically centred and positioned side by side to the camera having a 20 degree parallax.

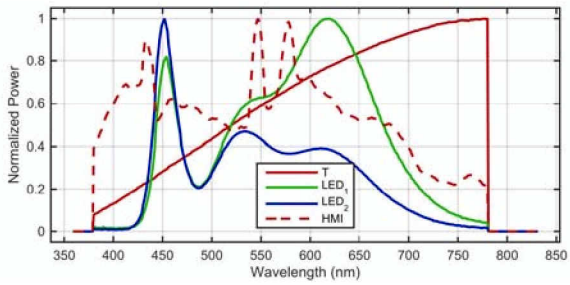

Figure 9. *SPDs of the different chart illuminations applied to chromaticity error minimisation*

Chromaticity Error. The original OFT responsivity (Figure 10, Origin) was compared to the improved responsivity that was estimated using chromaticity error minimisation. The responsivity based on a Tungsten chart illumination is illustrated in Figure 10, New). The chromaticities of all the ColorChecker patches were calculated using the spectral responsivities of both methods. Then for each, differences in patch chromaticities of the captured chart image were evaluated. Table 2 displays the mean values for chromaticity differences $\bar{\Delta}_k$ with $k = R,G,B$ for all patches for different estimated responsivities (OFT: the original

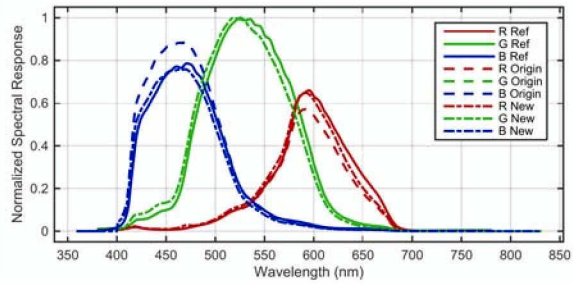

Figure 10. *Canon 5D Mark III responsivity comparison*

Table 2. *Mean chromaticity errors and standard deviations for the original method (OFT) and the adjusted responsivity estimation method for different chart illuminations evaluated to a Tungsten-illuminated chart*

	OFT/T	T/T	LED_1/T	LED_2/T	HMI/T
$\bar{\Delta}_r$	0.0360	0.0037	0.0043	0.0060	0.0085
$\bar{\Delta}_g$	-0.0046	0.0022	0.0029	0.0072	0.0010
$\bar{\Delta}_b$	-0.0314	-0.0059	-0.0072	-0.0132	-0.0095
σ_r	0.0117	0.0111	0.0112	0.0117	0.0110
σ_g	0.0088	0.0053	0.0052	0.0048	0.0049
σ_b	0.0150	0.0089	0.0092	0.0107	0.0098

Table 3. *Mean chromaticity errors and standard deviations for the adjusted responsivity estimation using Tungsten chart illumination and evaluated to a different illuminated chart*

	T/T	T/LED_1	T/LED_2	T/HMI
$\bar{\Delta}_r$	0.0037	0.0032	0.0009	-0.0014
$\bar{\Delta}_g$	0.0022	0.0022	-0.0022	0.0044
$\bar{\Delta}_b$	-0.0059	-0.0054	0.0013	-0.0030
σ_r	0.0111	0.0125	0.0143	0.0095
σ_g	0.0053	0.0097	0.0201	0.0051
σ_b	0.0089	0.0098	0.0125	0.0086

estimate; T, LED_1, LED_2, and HMI: responsivities obtained with chromaticity error minimisation for different illuminations) evaluated to the Tungsten-illuminated chart. The columns of Tables 2 and 3 represent the combinations of the applied responsivity to the evaluation of the chart under a certain illumination. The new method decreased the error by approximately one order of magnitude. Measured responsivities for all other tested camera models demonstrated comparable improvements. Additionally, Table 3 displays the results based on a chart illuminated with a Tungsten lighting but evaluated with different illuminated charts.

Comparison to the Monochromator Method. The responsivity of the new method (Figure 10, New) was compared to a monochromator-based measurement (Figure 10, Ref). The monochromator setup used a stabilized Tungsten light source with a CCT of 3400 K which illuminated a Czerny-Turner double monochromator. The entrance slit width of 1.5 mm ensured a full width half maximum of less than 10 nm for the spectral resolution. The monochromator used an echelette grating with 600 lines per mm and a blaze wavelength of 500 nm. After the 3 mm width exit slit, a collimator illuminated the entrance port of an integration sphere with a 10 cm diameter. Side by side, the camera and a spectroradiometer PR-670 for the reference measurement viewed into the sphere's output port at a distance of 15 cm. The spectroradiometer had a parallax of approximately 15 degrees. The images were captured at full aperture with ISO 100 with a five-second integration time. For the responsivity calculation, a centred circular region with a diameter of 200 pixels was first averaged. The sampling rate was from 380 to 780 nm with a 5 nm interval. The raw response was then normalised by the measured illumination power given by the spectroradiometer. First, for each channel the responsivity error e_k was calculated as follows:

$$e_k = \sqrt{\sum_{i=1}^{n} (S_{l,k}(\lambda_i) - S_{Ref,k}(\lambda_i))^2}, \tag{10}$$

where $l = Origin, New$ and designates the method to be compared with the reference. The mean error values $\bar{e}_k$ of ten measurements are given in the first three columns of Table 4. Second, the camera chromaticities were calculated for a set of objects j=1..m illuminated by a standard illuminant D65 as follows:

$$s_{k,j} = \sum_{i=1}^{n} \phi_{D65}(\lambda_i)\rho_j(\lambda_i)S_k(\lambda_i) / \sum_{i=1}^{n} \phi_{D65}(\lambda_i)S_k(\lambda_i). \tag{11}$$

Then for each object j, the Euclidian distance between the evaluated methods and the monochromator reference was calculated as

$$E_j = 255\sqrt{\Delta R^2 + \Delta G^2 + \Delta B^2}, \tag{12}$$

with $\Delta k = s_{j,k,l} - s_{j,k,Ref}$. This is the same error metric as described in [4], but here the spectral reflectance set consists of the ColorChecker patches together with all skin reflectances from [22]. The ColorChecker patches were chosen because this chart was used for the presented correction method. The selected skin reflectance, on the other hand, reflects the importance of correct skin tone reproduction for applications in photography and the movie industry. Percentile values of 50% (median), 80%, and 95% of the mean of ten measurements of the chromaticity differences are given in the right three columns of Table 4.

Table 4. *Mean errors and percentiles using responsivities given by the original and new methods compared to the monochromator-based responsivity*

	$\bar{e}_R$	$\bar{e}_G$	$\bar{e}_B$	50%	80%	95%
Origin	9.90	10.50	9.67	2.57	3.75	6.63
New	6.10	10.42	6.52	2.54	3.72	6.58

Reproducibility. The variability of the new method was evaluated for ten measurements during one year. Notably the last five measurements were done in one week. The slit-grating attachment was unmounted and disassembled between the measurements, and the ColorChecker chart and illumination source were repositioned every time. The chart was illuminated using the same Tungsten light with a manufacturer-specified CCT of 3400 K. Table 5 displays the mean value and standard deviation for the error.

Location Invariance. To test the sensitivity to spatial uniformity, the ColorChecker were additionally captured in all four quadrants (TL: top left, TR: top right, BL: bottom left, BR: bottom right) of the image. Table 6 displays the chromaticity errors for all positions of each channel for one Tungsten-illuminated

Table 5. Mean errors and standard deviation for the reproducibility test

$\bar{e}_R$	$\bar{e}_G$	$\bar{e}_B$	σ_{e_R}	σ_{e_G}	σ_{e_B}
6.10	10.42	6.52	0.69	0.90	0.98

sample. The results demonstrate that the chromaticity error minimisation approach is not influenced by inhomogeneous illumination or lens vignetting effects, and thus the method is location invariant, and a vignetting correction for the chart image is not required.

Table 6. Errors for different chart locations

	e_R	e_G	e_B
Centre	6.155	10.945	6.657
TL	6.163	10.945	6.722
TR	6.098	10.944	6.996
BL	6.099	10.944	6.858
BR	6.160	10.945	6.652

Different Chart Illumination. The algorithm was tested using different chart illuminations. The evaluation results are displayed in Table 7 and have similar errors. Furthermore, an additional evaluation of the algorithm was conducted. The chromaticity sets for the four illuminations were combined in order to extend the equation system of Equation 8 for multiple charts under different illuminations. No significant improvement in the recovery of responsivity was observed. Also, the method was tested without measuring SPDs but instead using an SPD of the vendor-specified standard illuminant equivalent instead. For Tungsten illumination this led to acceptable results, but especially for the LED light source, the estimated responsivities were insufficient.

Table 7. Errors for different chart illuminants

	e_R	e_G	e_B
T	6.155	10.945	6.657
LED_1	6.157	10.945	6.748
LED_2	6.136	10.944	7.938
HMI	6.371	10.945	6.868

Error in Colour Appearance

Usually, at least in movie and print productions, the camera-caught images are presented to the human observer. The camera signals are transformed into colorimetric CIE-XYZ values using the conversion Matrix M given by Equation 2. This results in incorrect colour tristimulus vaues that are additionally caused by the errors of the applied responsivity. The colour appearance can then be evaluated by transforming the CIE-XYZ values in a colour appearance model (CAM) domain, for example CIE-Lab76 or CIECAM02. The discussion of CAM domain-based errors is more appropriate in visualisation. Therefore, an evaluation was conducted on applying the responsivities of the proposed method that uses the captured chart image of the additional chromaticity error minimisation step. A conversion matrix M was estimated using the method from [14], which defines a standard in the movie industry for camera colour characterisation. The evaluation applies the ColorChecker patches reflectance set, a Tungsten scene illuminant and a chromatic adaptation to a standard daylight D50 using the Bradford matrix for chromatic adaptation transform. The function f_{CAM} was chosen to convert the CIE-XYZ tristimuli to CIE-Lab76 to minimise the mean perceptual error. The resulting conversion matrix was then applied to convert the ColorChecker patches. For all patches the CIEDE2000 values were calculated using the CIE-Lab76 reference values and the matrix transformation-based values. The mean CIEDE2000 values were less then $\approx$0.55 for the measured cameras.

Measured Spectral Responsivities Data Set

Table 8. Cameras of responsivities data set

Machine Vision Baumer TXG50c, FLIR PG Flea
Photo Canon 5DMarkIII/6D, Nikon D800/D750, Sony A7R
Movie ARRI Alexa, Blackmagic PC 4k, GoPro 4+

Table 8 gives an overview of the measured cameras sorted by application. Three samples from machine vision, photography (Photo), and cinematography (Movie) are shown in Figure 11: a FLIR Point Grey Research - Flea3 FL3-U3-32S2C with a Pentax 1.2/6 lens (PG Flea), a Nikon D800 with a PC-E Micro Nikkor 45mm f/2.8D ED (Nikon D800), and a BlackMagic Design Production Camera 4K with a Canon EF 24-70mm f/2.8L II USM lens (BM PC 4k). The dataset for all measured samples, including the SPDs, the diffraction spectrum images, the captured chart, an XML file describing lenses and measurement conditions, and the derived responses is published at [23].

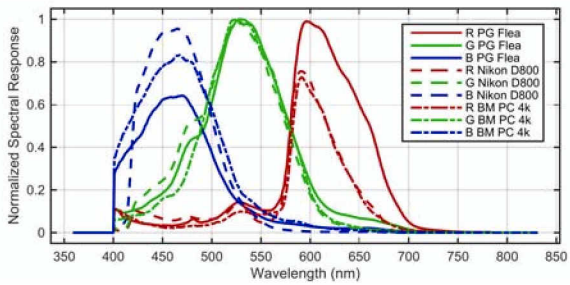

Figure 11. Selected samples of measured responsivities

Conclusion

An improved camera spectral responsivity measurement method was presented. It combines the direct measurement of the spectral response with a chart-image-based response adjustment using a chromaticity error minimisation based correction step. This method significantly reduces the error of the estimated response compared to the original method. In particular, it reduces observed wide-ranging differences of lens and sensor vignetting effects, errors of spectroradiometer measurements of reference SPDs, and errors induced by the slit-grating attachment. The algorithm produces reproducible results and is location and illumination invariant. Camera responses given by the improved procedure were used to estimate colour transformation matrices. The

application of these matrices demonstrated robust results with acceptable mean colour appearance differences of CIEDE2000, less then 0.55 compared to the reference colours. A dataset was created applying the presented procedure that includes the required input dataset for the algorithm as well as estimated responsivities for cameras from machine vision, photographic, and cinematographic applications. The presented method offers a robust responsivity estimation using an inexpensive slit-grating attachment and a widely used colour chart. It provides camera response measurement access for a wider audience in colour science studies and applications.

Acknowledgements

We would like to thank the Institute of Applied Optics and the Institute of Space Systems at the Space Center Baden-Württemberg, both at the University of Stuttgart, for using their optical laboratories. This work was supported by *Kooperatives Promotionskolleg Digital Media* at Stuttgart Media University and the University of Tübingen.

References

[1] P. M. Hubel, D. Sherman, and J. E. Farrell, "A Comparison of Methods of Sensor Spectral Sensitivity Estimation," in *Proc. 2nd IS&T Color Imaging Conf.*, vol. 1994, pp. 45–48, Society for Imaging Science and Technology, 1994.

[2] D. S. Hawkins and P. Green, "Spectral Characterisation of a Digital Still Camera through a Single Integrating Exposure," in *Conf. on Colour in Graphics, Imaging, and Vision*, vol. 2008, pp. 477–480, Society for Imaging Science and Technology, 2008.

[3] J. M. DiCarlo, G. E. Montgomery, and S. W. Trovinger, "Emissive Chart for Imager Calibration," in *Proc. 12th IS&T Color Imaging Conf.*, vol. 2004, pp. 295–301, Society for Imaging Science and Technology, 2004.

[4] L. W. MacDonald, "Determining Camera Spectral Responsivity with Multispectral Transmission Filters," in *Proc. 23rd IS&T Color Imaging Conf.*, vol. 2015, pp. 12–17, Society for Imaging Science and Technology, 2015.

[5] M. Rump, A. Zinke, and R. Klein, "Practical Spectral Characterization of Trichromatic Cameras," in *Proceedings of the 2011 SIGGRAPH Asia Conference*, SA '11, (New York, NY, USA), pp. 170:1–170:10, ACM, 2011.

[6] J. Jiang, D. Liu, J. Gu, and S. Süsstrunk, "What is the Space of Spectral Sensitivity Functions for Digital Color Cameras?," in *2013 IEEE Workshop on Applications of Computer Vision (WACV)*, pp. 168–179, Institute of Electrical and Electronics Engineers, Jan 2013.

[7] S. Han, Y. Matsushita, I. Sato, T. Okabe, and Y. Sato, "Camera spectral sensitivity estimation from a single image under unknown illumination by using fluorescence," in *2012 IEEE Conference on Computer Vision and Pattern Recognition*, pp. 805–812, Institute of Electrical and Electronics Engineers, June 2012.

[8] A. Karge, "Open Film Tools - a Free Toolset for a Spectral Data Based Movie Camera Colour Characterization," in *22. Workshop Farbbildverarbeitung Ilmenau*, vol. 2016, 2016.

[9] R. Luther, "Aus dem Gebiet der Farbreizmetrik," *Zeitschrift für Technische Physik*, vol. 8, pp. 540–558, 1927.

[10] G. D. Finlayson and M. S. Drew, "White-Point Preserving Color Correction," in *Proc. 5th IS&T Color Imaging Conf.*, vol. 1997, pp. 258–261, Society for Imaging Science and Technology, 1997.

[11] G. Hong, M. R. Luo, and P. A. Rhodes, "A Study of Digital Camera Colorimetric Characterisation based on Polynomial Modelling," *Color Research and Application*, vol. 26, no. 1, pp. 76–84, 2001.

[12] G. D. Finlayson, M. Mackiewicz, and A. Hurlbert, "Root-Polynomial Colour Correction," in *Proc. 19th IS&T Color Imaging Conf.*, vol. 2011, pp. 115–119, Society for Imaging Science and Technology, 2011.

[13] M. Mackiewicz, C. F. Andersen, and G. D. Finlayson, "Hue Plane Preserving Colour Correction using Constrained Least Squares Regression.," in *Proc. 23rd IS&T Color Imaging Conf.*, vol. 2015, pp. 18–23, Society for Imaging Science and Technology, 2015.

[14] AMPAS P-2009-001, "Recommended Procedures for the Creation and Use of Digital Camera System Input Device Transforms (IDTs)," Standard, Academy of Motion Picture Arts and Sciences, Los Angeles, USA, 2012.

[15] J. W. Draper, *A Treatise on the Forces which Produce the Organization of Plants: With an Appendix, Containing Several Memoirs on Capillary Attraction, Electricity, and the Chemical Action of Light.* Harper & Brothers, 1844.

[16] H. Draper, "Liv. On Diffraction-Spectrum Photography," *The London, Edinburgh, and Dublin Philosophical Magazine and Journal of Science*, vol. 46, no. 308, pp. 417–425, 1873.

[17] U. Krüger, "Bestimmung ausgewählter Parameter und Kennwerte digitaler Kamerasysteme," *PHOTONIK STUTTGART*, vol. 38, no. 2, p. 66, 2006.

[18] M. Leonhardt and H. Brendel, "Critical Spectra in the Color Reproduction Process of Digital Motion Picture Cameras," in *Proc. 23rd IS&T Color Imaging Conf.*, vol. 2015, pp. 167–170, Society for Imaging Science and Technology, 2015.

[19] A. Savitzky and M. J. Golay, "Smoothing and Differentiation of Data by Simplified Least Squares Procedures," *Analytical chemistry*, vol. 36, no. 8, pp. 1627–1639, 1964.

[20] M. Aggarwal, H. Hua, and N. Ahuja, "On Cosine-Fourth and Vignetting Effects in Real Lenses," in *Proceedings Eighth IEEE International Conference on Computer Vision. ICCV 2001*, vol. 1, pp. 472–479 vol.1, Institute of Electrical and Electronics Engineers, 2001.

[21] D. B. Goldman and J.-H. Chen, "Vignette and exposure calibration and compensation," in *Tenth IEEE International Conference on Computer Vision (ICCV'05) Volume 1*, vol. 1, pp. 899–906 Vol. 1, Institute of Electrical and Electronics Engineers, Oct 2005.

[22] ISO/TR 16066:2003(E), "Graphic Technology Standard Object Colour Spectra Database for Colour Reproduction Evaluation," Standard, International Organization for Standardization, Geneva, CH, 2003.

[23] A. Karge and I. Rieger, "Database of spectral spectral responsivities of cameras." `https://www.hdm-stuttgart.de/open-film-tools/english/camera_responsivities`, November 2018.

Author Biography

Andreas Karge (born 1971 in Halle/Saale, Germany) is a PhD researcher at the University of Tübingen and Stuttgart Media University. He investigates spectral-data-based colour correction methods for imaging devices. Besides he works as a software engineer at GMG GmbH & Co KG in Tübingen, developing algorithms for colour profile creation and image processing. Andreas Karge received his engineering degree in imaging sciences and media technology (2001) and an M.Sc. in media informatics (2005) from the University of Applied Sciences Cologne.